

OPEN

Anatomic Localization and Compression Points of Occipital Nerves: Therapeutic Insights Using K-Means and Cadaveric Atlas

Thania de Oca Mora, MD , Jonathan Samuel Zúñiga-Cordova, MD[‡], Carlos Castillo-Rangel, MD ^{*}, Gerardo Marín, MD, PhD [§],
Cristofer Zarate-Calderon, PhD ^{||}, Pedro G. L. B. Borges, MD [¶], Ariana Tejeda Santiz, BSc[#], Julio César Pérez Cruz, MD^{**},
Valeria Forlizzi, MD ⁺⁺, Daniel Oswaldo Davila-Rodriguez, MD^{*}, Matías Baldoncini, MD ⁺⁺

^{*}Department of Neurosurgery, "Hospital Regional 1° de Octubre", Instituto de Seguridad y Servicios Sociales de los Trabajadores del Estado, Mexico City, Mexico; [‡]Department of Vascular Neurosurgery, Centro Médico Nacional "20 de Noviembre", Instituto de Seguridad y Servicios Sociales de los Trabajadores del Estado, Ciudad de México, Mexico; [§]Neural Dynamics and Modulation Lab, Cleveland, Ohio, USA; ^{||}Department of Biophysics, Brain Research Institute, Universidad Veracruzana, Xalapa, Veracruz, Mexico; [¶]D'Or Institute for Research and Education Rua Diniz Cordeiro, Rio de Janeiro, RJ, Brazil; [#]Faculty of Statistics and Informatics, Universidad Veracruzana, Xalapa, Veracruz, Mexico; ^{**}Laboratorio de Técnicas Anatómicas y Material Didactico, Escuela Superior de Medicina, Instituto Politécnico Nacional, Mexico City, Mexico; ⁺⁺Laboratorio de Neuroanatomía Microquirúrgica, Segunda Cátedra de Anatomía, Universidad de Buenos Aires, Buenos Aires, Argentina; ⁺⁺Department of Neurological Surgery, Hospital San Fernando, Buenos Aires, Argentina

Correspondence: Gerardo Marín Márquez, Neural Dynamics and Modulation Lab, 9500 Euclid Ave, Cleveland, OH 44196, USA. Email: drmarin.neuroscience@gmail.com

Received, August 14, 2024; **Accepted,** January 15, 2025; **Published Online,** April 29, 2025.

Operative Neurosurgery 00:1–9, 2025

<https://doi.org/10.1227/ons.0000000000001598>

Copyright © 2025 The Author(s). Published by Wolters Kluwer Health, Inc on behalf of Congress of Neurological Surgeons. This is an open access article distributed under the terms of the Creative Commons Attribution-Non Commercial-No Derivatives License 4.0 (CCBY-NC-ND), where it is permissible to download and share the work provided it is properly cited. The work cannot be changed in any way or used commercially without permission from the journal.

BACKGROUND AND OBJECTIVES: The greater occipital nerve (GON) and lesser occipital nerve (LON) have gained importance because of conditions such as occipital neuralgia and cervicogenic headaches. To a great depth, their anatomy is essential for performing viable diagnostic and therapeutic procedures such as nerve blocks and decompression procedures. This research involves identifying key anatomic landmarks and the potential compression points of the GON and LON using cadaveric dissections for possible surgical approaches.

METHODS: Five fresh, untreated cadavers, 3 male and 2 female, were dissected bilaterally to trace the pathways of the GON and LON. Anatomic measurements were made using ImageJ software, and coordinates were analyzed with K-means clustering for optimal intervention points. These dissections focused on determining in detail the relation of these nerves to surrounding muscular and fascial structures.

RESULTS: The study shows that for GON, there were many points possible for compression, such as where it pierced through the semispinalis and trapezius muscles along the course of the occipital artery. For the LON, however, the potential compression sites were contact points along the course of the occipital artery. After applying K-means clustering, 4 centroids (M1, M2, M3, and M4) were identified. M1 and M3 correspond to the LON, while M2 and M4 correspond to the GON. These centroid locations lie near the nerves' most common compression sites, suggesting they could serve as strategic landmarks for surgical approaches. Cluster quality measures (inertia and silhouette coefficients) showed well-defined clusters.

CONCLUSION: This study yields anatomic information about the GON and LON anatomy and illustrates key compression points and optimal sites for therapeutic interventions. Within the constraints of sample size, these findings provide preliminary anatomic insights that can guide more precise nerve block and decompression techniques for occipital neuralgia and related headaches.

KEY WORDS: Occipital nerve, Occipital neuralgia, Microsurgical anatomy, Neuroanatomic dissection

The greater occipital nerve (GON) and lesser occipital nerve (LON) traverse the posterior part of the scalp and neck as dorsal branches of the spinal cervical plexus.¹ The GON is

the medial branch of the posterior division of C2, although it may also receive some fibers from the dorsal ramus of spinal nerve C3.² It subsequently pierces the trapezius muscle to join the occipital

ABBREVIATIONS GON, greater occipital nerve; LON, lesser occipital nerve.

Supplemental digital content is available for this article at operativeneurosurgery-online.com.

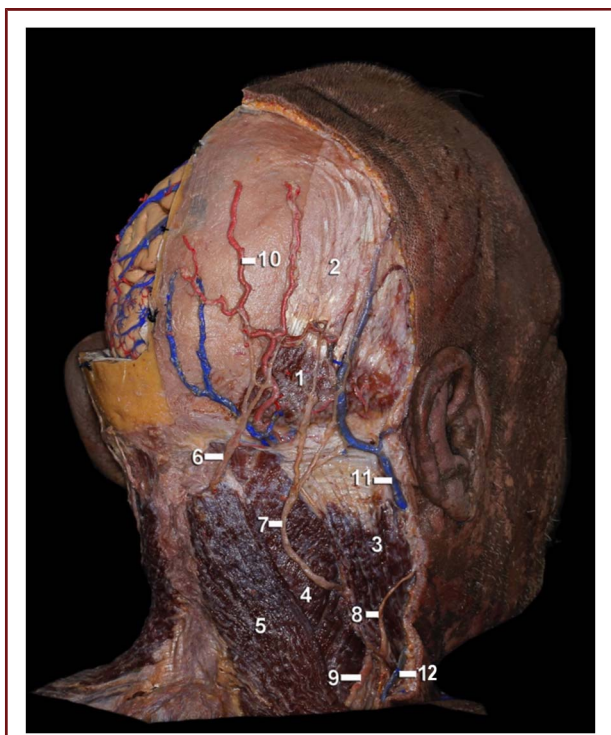


FIGURE 1. Muscles: 1, occipital belly of the occipitofrontal muscle, 2, epicranial aponeurosis, 3, sternocleidomastoid, 4, splenius, 5, trapezius. Nerves: 6, greater occipital, 7, lesser occipital nerve, 8, greater auricular, 9, spinal portion of the accessory nerve. Vessels: 10, occipital artery, 11, posterior auricular vein, 12, external jugular vein.

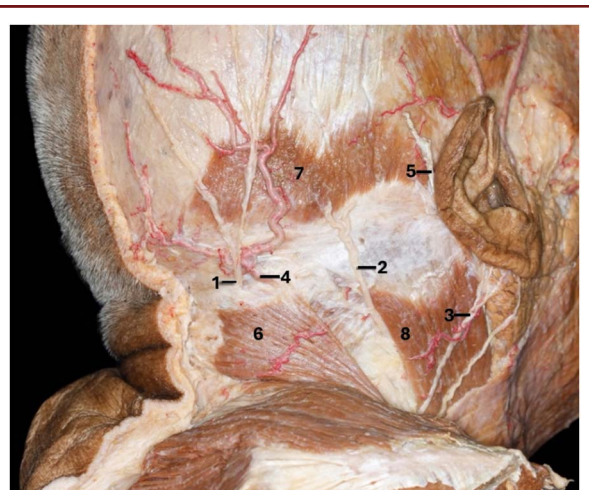


FIGURE 2. Posterolateral region of the head and neck. 1, Greater occipital nerve, 2, lesser occipital nerve, 3, greater auricular nerve, 4, occipital artery, 5, posterior auricular vein, 6, trapezius muscle, 7, occipital belly of the occipitofrontal muscle, 8, sternocleidomastoid muscle.

artery's course, branching to innervate the posterior scalp (Figure 1). The LON, arising from the posterior divisions of C2 and C3, lies lateral to the GON. It crosses the sternocleidomastoid muscle and courses superolaterally toward the posterior auricle, as shown in Figure 2, where it crosses inferiorly near the mandibular angle.

Understanding the course of these nerves is essential. Accurate descriptions of their topographic anatomy and anatomic variations are crucial for diagnosing and planning therapeutic procedures for occipital neuralgia, Arnold headache, cervicogenic headaches, and cluster headaches.^{1,3} This includes diagnostic or therapeutic nerve blocks and neurolysis of the GON. Procedures such as percutaneous radiofrequency denaturation, rhizotomy, C2 spinal nerve ganglionectomy, cryotherapy, or decompression for entrapment rely on understanding possible entrapment points along their course through the neck muscles.⁴⁻⁶ More than anatomic references are needed for this task. Not only is palpation of reference through the skin not precise enough but several anatomic variations have also been described along the course of the GON.¹

Clinically, the diagnosis of GON or LON compression is often established through focused history, physical examination, and diagnostic nerve blocks. Patients typically present with occipital-region

pain reproduced by palpation along the nerve's trajectory, temporary symptom relief after a nerve block supports the diagnosis. Imaging modalities such as ultrasound or MRI can visualize nerve thickening or entrapment at specific anatomic locations.⁷⁻⁹

Therefore, the aim of this article was to determine the anatomic-topographic points of the GON and LON through cadaveric dissections and elucidate their relationships with the neck, semispinalis, and trapezius muscles. By examining the size, location, trajectory, distribution, and anatomic variations of these nerves, we aim to establish precise reference points for surgical interventions, providing practical applications for the treatment of headache-associated pathologies.

METHODS

Dissections were conducted in a specialized neuroanatomy laboratory in a university's anatomy department. The study received ethical approval from the Clinical and Research Bioethics Committee of the University of Buenos Aires (Approval Number: 27345/7, Resolution No. 3145).

Permission for the use and publication of cadaveric materials and images was obtained as part of the ethical approval process. Informed consent was not applicable because the study involved cadaveric specimens and nonliving patients.

We used 5 fresh cadavers (3 male and 2 female), dissected bilaterally, and also included specimens prepared with latex injection for better vascular visualization. These latex-injected specimens were perfused and fixed with a 10% formaldehyde solution (*Sigma-Aldrich*) administered by an infusion pump (*Portiboy Mark IV; The Dodge Company*). White latex (*Poliformas Plásticas*) was mixed with acrylic paint (*Politec*)—carmine 319 for arteries and ultramarine blue 315 for veins—in a 1:1 ratio. For more technical details on the latex injection procedure, see **Supplemental Digital Content 1** [<http://links.lww.com/ONS/B190>].

All microsurgical procedures were performed using microdissection instruments and an operating microscope. The occipital and suboccipital regions were carefully reviewed to identify the GON and LON, along with potential compression points.

Dissection Protocol

The fresh cadavers were positioned prone. After a suboccipital trichotomy, a linear incision was made from theinion to the second cervical vertebra, exposing the superior nuchal line as well as the fascia of the sternocleidomastoid and trapezius muscles. The GON and LON were identified along their trajectories, and the process was documented with photographs (Figure 3). The suboccipital triangle was accessed by blunt dissection, and the muscles forming this region were individually exposed, removing adipose tissue and venous plexuses for clear visualization of the nerves and their vascular relationships. An exhaustive list of instruments used is provided in **Supplemental Digital Content 1** [<http://links.lww.com/ONS/B190>].

All dissections and measurements were performed by a single evaluator, a fellowship-trained neuroanatomist with over 6 years of experience, under the supervision of a vascular neurosurgeon. This approach ensures consistency in measurements and reduces the risk of inter-rater discrepancy.

Identification of Potential Compression Sites

After exposing the GON and LON, potential compression sites were determined. We primarily looked for areas where the nerve diameter visibly decreased as the nerve traversed dense fascial planes or passed between muscle and fascial boundaries, specifically, (1) through the fascia of the oblique and semispinalis muscles, where the nerve is surrounded by a layer of dense connective tissue; (2), (3) at the entrance and exit to the semispinalis muscle, where the nerve is compressed by the junction of the muscle and the surrounding fascia; (4), (5) at the entrance and exit to the trapezius muscle, where the nerve is compressed by the junction of the muscle and the surrounding fascia; and (6) in the region of the occipital artery, where the nerve is compressed by the artery and the surrounding fascia.

These observations match descriptions in anatomic and clinical studies, which also report up to 6 compression points associated with occipital neuralgia. In our cadaveric analysis, we found that both the GON and LON can be compressed where they perforate dense fascial layers and at sites where the occipital artery intersects or closely abuts the nerve.^{2,10,11}

Measurements

The landmarks are shown in Figure 4, and their classification, including anatomic measurements (A–K), is presented in **Supplemental Digital Content 1** [<http://links.lww.com/ONS/B190>].

Statistical Analysis

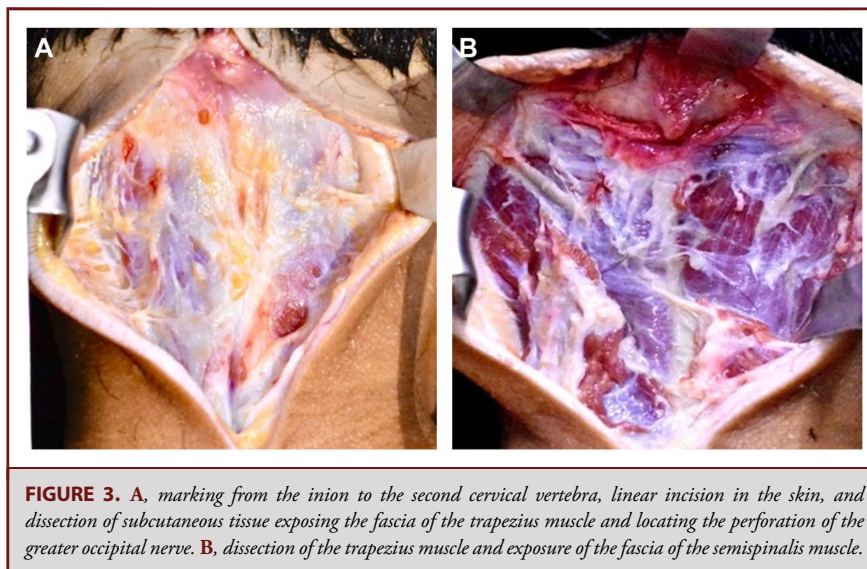
We used the Mann-Whitney *U* test to compare variables by sex (male/female) and by age group (older/younger than 21 years), assuming non-normal data distribution because of the small sample size. To compare the left and right sides within each cadaver, the Wilcoxon signed-rank test was performed. Significance was set at $P < .05$. We calculated mean values and 95% CIs for each parameter (A–K) across age and sex categories. The data analysis was conducted in Python 3.

K-Means

We applied an unsupervised learning model, the K-means algorithm, to identify the optimal anatomic points for surgical intervention. The methods and parameters are present in **Supplemental Digital Content 2** [<http://links.lww.com/ONS/B191>]. This statistical approach enabled us to accurately identify compression points in the GON and LON nerves, thereby optimizing techniques for nerve block and decompression.^{12,13}

RESULTS

Ten sides from 5 cadavers underwent dissection. The average age of the cadavers was 57 years (range: 16–79 years), comprising 3 male cadavers and 2 female cadavers. All heads were dissected bilaterally.



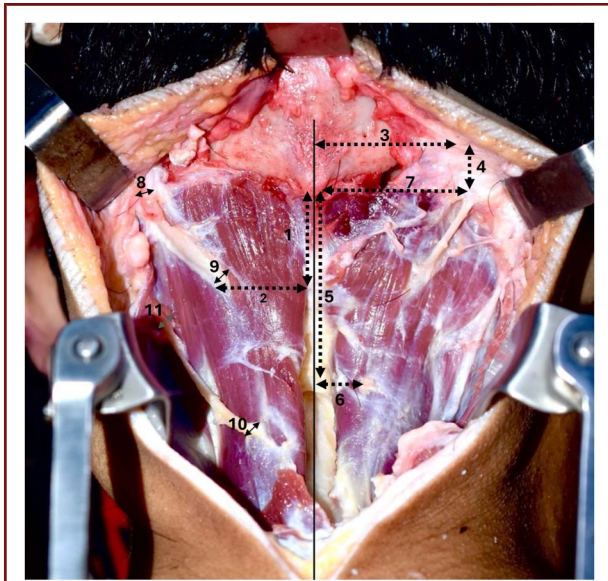


FIGURE 4. Reference points are taken in cadaveric dissections. 1, Distance from the midline to the level where the GON pierces the semispinalis muscle to the occiput. 2, Distance from the midline to the point where the GON pierces the semispinalis muscle. 3, Distance from the midline to where the GON crosses the nuchal line. 4, Distance from the nuchal line to where the GON pierces the trapezius muscle. 5, A horizontal line is drawn toward the midline from where the LON pierces the semispinalis muscle, and then the distance to the occiput is measured. 6, Distance from the midline to the point where the GON pierces the right and left semispinalis muscles. 7, Distance from the midline to the point where the LON pierces the trapezius muscle. 8, Width of the GON where it pierces the trapezius muscle. 9, Width of the GON on the surface of the semispinalis muscle. 10, Width of the LON on the surface of the semispinalis muscle. 11, Width of the LON on the surface of the sternocleidomastoid muscle. GON, greater occipital nerve; LON, lesser occipital nerve.

General Observations and Demographic Subanalysis

No statistically significant differences were found in the measured distances between male (n = 3) and female (n = 2) cadavers across reference points (A–K) (U = 3.0, *P* > .05, 95% CI: 16.03-17.64). Similarly, there was no significant correlation between age (younger than 21 years) and measured distances (U = 4.0, *P* > .05, 95% CI: 15.09-17.65). These findings suggest that neither age nor sex had a notable effect on the measurements of the parameters examined. The GON was identified in most cases, perforating the fascia of the trapezius muscle and, subsequently, the semispinalis muscle. The LON was identified at the posterior border of the sternocleidomastoid muscle, except in 1 case where it pierced the semispinalis muscle before running along the posterior border of the sternocleidomastoid muscle. No LON fascial or muscular compression was observed at its exit point. However, in some cadavers, contact with different portions of the course of the occipital artery was observed (Figures 5 and 6).

Greater Occipital Nerve and Lesser Occipital Nerve Trajectories

Up to 6 possible compression sites were described for GON. For the LON, no fascial or muscular compression was observed at its exit, but we did document possible contact points with the occipital artery (Figure 7).

Measurements and Observed Variation

Measurements were conducted according to the parameters established in Figure 4, and the results are presented in Tables 1 and 2. The coordinates were established based on a Cartesian plane, where the intersection of the X and Y axes is the occipital protuberance, the X axis is the superior nuchal line, and the Y axis is the midline from the occipital protuberance to the second cervical vertebra (Figure 8).

No significant side-to-side differences were found (*P* > .05, Wilcoxon test), although isolated outliers highlight the necessity of increasing the sample size to better characterize anatomic variability. Despite this, individual outliers emphasize the importance of increasing the sample size to establish normative values and better characterize anatomic variations.

K-Means Clustering and Intervention Points

The coordinates corresponding to point M1 represent the location of the LON, whereas the coordinates of M3 also represent the LON. The coordinates of M4 indicate the location where the GON pierces the semispinalis muscle and a coordinate below the LON location. The M2 coordinates represent the site where the GON crosses the superior nuchal line and the points where the GON crosses the superior nuchal line.

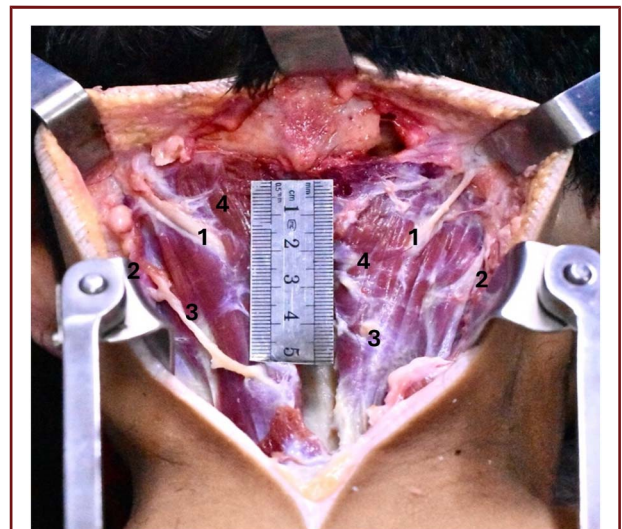


FIGURE 5. Fresh cadaveric dissection number 1. 1, Greater occipital nerve, 2, retracted trapezius muscle, 3, lesser occipital nerve, 4, semispinalis muscle.

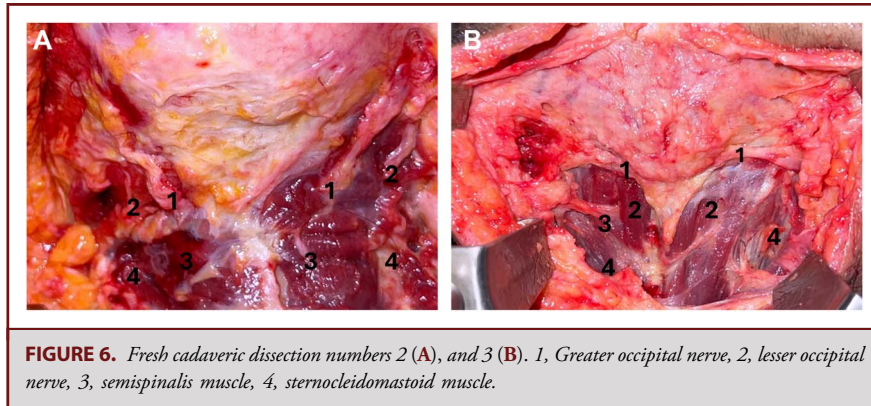


FIGURE 6. Fresh cadaveric dissection numbers 2 (A), and 3 (B). 1, Greater occipital nerve, 2, lesser occipital nerve, 3, semispinalis muscle, 4, sternocleidomastoid muscle.

According to the K-means clustering, the intervention points are as follows: M1 is located 3.90 cm lateral to the superior nuchal line and 3.25 cm below it. M2 is located 3.34 cm from the beginning of the superior nuchal line and 0.31 cm below it. M3 is located 1.50 cm from the superior nuchal line and 4.40 cm below it. M4 is located at the point where the GON pierces the semispinalis muscle, 1.55 cm from the superior nuchal line and 2.05 cm below it (Figure 8).

To evaluate the quality of the formed clusters, we used 2 widely recognized metrics: inertia and the silhouette coefficient. We determined an inertia of 40.709 and a silhouette coefficient of 0.552. These M points reflect common locations of the GON and LON rather than exclusively compression sites. Although points M1 and M3 did not coincide with overt compressive anatomies in our sample, they represent consistent landmarks where the LON may be accessed for diagnostic or therapeutic interventions. Similarly, M2 and M4 represent frequent anatomic reference points for GON. Although our findings are preliminary and

limited by the small sample size, they underscore the importance of recognizing anatomic variations and potential nerve compression sites, especially in procedures such as neurectomy, decompression, and nerve block interventions.

DISCUSSION

The GON and LON are vital for the sensory innervation of the posterior scalp and neck, playing crucial roles in diagnosing and treating conditions such as occipital neuralgia and cervicogenic headaches. The GON, originating from the dorsal ramus of C2 (and sometimes C3), travels through multiple muscle layers to innervate the posterior scalp and ear. The LON arises from the ventral ramus of C2 (occasionally C3) and provides sensory input to the upper ear and lateral neck. Understanding the detailed anatomy of these nerves is essential for effective nerve blocks and decompression procedures.^{14,15}

This study aimed to enhance the anatomic-topographic localization of GON and LON from their origins in the cervical plexus to their pathways in sensory innervation of the upper back, neck, and scalp. We identified several potential compression points for GON, including its entry and exit through the semispinalis muscle, entry into the trapezius muscle, insertion of the trapezius muscle, and along the occipital artery. Similarly, possible compression points for the LON were found along the trajectory of the occipital artery, aligning with previous medical literature.¹⁶ The precise localization of these points can aid in planning decompression procedures to treat different headache etiologies involving the occipital nerve plexus.

Our work proposes 2 potential intervention points each for GON and LON based on observations from 5 cadavers and 10 dissections. These points are applicable in corticosteroid injections, which have been investigated for treating occipital neuralgia and episodic and chronic cluster headaches.¹⁷⁻¹⁹

The role of GON in treating cluster headaches is likely related to its convergence with the trigeminal and second-order nociceptors in the trigeminal caudalis nucleus.²⁰ For this, treatments with corticosteroid injections can decrease trigeminal pain

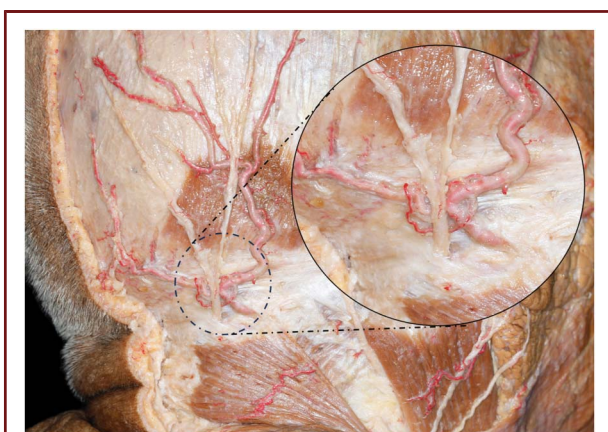


FIGURE 7. Fresh cadaveric dissection number 4. Posterolateral region of the head and neck and compression points by the occipital artery and trapezius muscle.

TABLE 1. Measurements and Averages in Millimeter of Reference Points Taken in Cadaveric Dissections

Reference points Sex (age)	Left head (mm)					Mean	95% CI
	1 M (16)	2 F (73)	3 M (55)	4 M (64)	5 F (79)		
A	24.92	25.77	12.33	24	19.33	21.27	13.03-25.69
B	18.23	19.42	11.21	9.49	14.79	14.63	9.66-19.30
C	43.93	30.97	30.27	31.52	33.41	34.02	30.34-42.88
D	4.35	5.38	4.85	8.15	5.44	5.63	4.40-7.88
E	54.71	44.43	23.91	30.64	36.2	37.98	24.58-53.68
F	10.88	18.26	19.59	43.15	15.09	21.39	11.30-40.79
G	39.06	31.53	33.25	24.2	34.03	32.41	24.93-38.56
H	3.48	3.69	3.67	4.17	3.84	3.77	3.50-4.14
I	2.86	4.9	4.72	2.23	3.16	3.57	2.29-4.88
J	2.68	2.23	3.67	1.99	2.48	2.61	2.01-3.57
K	2.32	2.19	3.17	3.19	2.67	2.71	2.20-3.19

Reference points Sex (age)	Right head (mm)					Mean	95% CI
	1 M (16)	2 F (73)	3 M (55)	4 M (64)	5 F (79)		
A	21.44	19.61	8.22	31.41	22.89	20.71	10.38-31.05
B	25.91	17.5	14.03	6.9	18.86	16.64	8.01-25.27
C	41.24	40.96	35.68	22.69	37.19	35.55	26.14-44.96
D	8.29	4.61	9.72	7.99	5.14	7.15	4.44-9.86
E	44.15	28.27	42.61	39.03	33.01	37.41	29.13-45.70
F	12.85	31.53	19.06	55.84	27.45	29.35	8.87-49.83
G	39.69	41.15	35.68	20.83	25.49	32.57	21.43-43.71
H	2.15	5.3	3.73	4.24	3.22	3.73	2.27-5.18
I	1.78	4.2	4.85	2.54	2.06	3.09	1.40-4.78
J	2.34	3.4	3.36	2.58	3.01	2.94	2.35-3.52
K	1.09	3.6	2.77	3.32	3.05	2.77	1.54-3.99

A. Distance from the midline to the level where the GON perforates the semispinalis capiteis muscle at the occiput. B. Distance from the midline to the point where the GON perforates the semispinalis capitis muscle. C. Distance from the midline to where the GON crosses the nuchal line. D. Distance from the nuchal line to the site where the GON perforates the trapezius muscle. E. A horizontal line is drawn toward the midline from where the LON perforates the semispinalis capitis muscle, and subsequently, the distance to the occiput is measured. F. Distance from the midline to the point where the GON perforates the right and left semispinalis capitis muscle. G. Distance from the midline to the point where the LON perforates the trapezius muscle. H. Width of the GON where it perforates the trapezius. I. Width of the GON on the surface of the semispinalis capitis muscle. J. Width of the LON on the surface of the semispinalis capitis muscle. K. Width of the LON on the surface of the sternocleidomastoid muscle. No statistically significant differences between the left and right-sided structures of the dissected cadavers were observed. F, female; GON, greater occipital nerve; LON, lesser occipital nerve; M, male.

through unmyelinated nerve fibers.²¹ In the study by Brandt et al,³ corticosteroid infiltration relieved symptoms of medically intractable chronic cluster headache in 69%, 68%, and 82% of patients after 1, 2, and 3 infiltrations, respectively.

Won et al¹⁴ detailed the topographical relationships between GON, trapezius muscle, and occipital artery, identifying key landmarks such as the external occipital protuberance and the occipital artery as critical for accurately locating GON during

TABLE 2. Determination of the Points in the Cartesian Plane

ID	Point (x, y)	ID	Point (x, y)	ID	Point (x, y)	ID	Point (x, y)
C1	(3.9, 0)	GD1	(4.3, -0.4)	EF1	(1.08, -5.4)	AB1	(1.8, -2.4)
C2	(3.15, 0)	GD2	(3.09, -0.53)	EF2	(1.8, -4.4)	AB2	(1.9, -2.5)
C3	(3.32, 0)	GD3	(3, -0.4)	EF3	(1.9, -2.3)	AB3	(1.1, -1.2)
C4	(2.42, 0)	GD4	(3.1, -0.8)	EF4	(4.3, -3)	AB4	(0.9, -2.1)
C5	(3.96, 0)	GD5	(3.3, -0.54)	EF5	(1.5, -3.6)	AB5	(1.4, -1.9)
C6	(4.15, 0)	GD6	(4.1, -0.8)	EF6	(1.2, -4.4)	AB6	(2.5, -2.1)
C7	(3.56, 0)	GD7	(4, -0.46)	EF7	(3.1, -2.8)	AB7	(1.7, -1.9)
C8	(2.02, 0)	GD8	(3.5, -0.97)	EF8	(1.9, -4.2)	AB8	(1.4, -0.82)
C9	(3.4, 0)	GD9	(2.2, -0.78)	EF9	(5.5, -3.9)	AB9	(0.6, -3.1)
C10	(2.54, 0)	GD10	(3.7, -0.51)	EF10	(2.7, -3.3)	AB10	(1.8, -2.2)

The intersection of the X and Y axes is the occipital protuberance; the X axis is the superior nuchal line, and the Y axis is the midline from the occipital protuberance to the second cervical vertebra.

nerve injections. These studies support our findings and underscore the necessity of precise anatomic knowledge for effective treatment planning.

Various block points for GON have been proposed in the literature. Bovim et al²² described a block point approximately 2 cm lateral and 2 cm below the external occipital protuberance. Similarly, Ashkenazi and Levin suggested a point 3.5 cm inferolaterally to the external occipital protuberance, while Natsis et al proposed a location 2.0 to 2.5 cm below the external occipital protuberance and approximately 1.5 cm lateral to the midline.^{1,23} These proposed points are consistent with our identified points M2 and M4, reinforcing their usefulness in clinical practice. The infiltration points for GON showed low mean square errors, indicating their potential effectiveness for treatment.

On the other hand, LON presents more variability, complicating the determination of precise intervention points. Lucas et al provided a detailed anatomic description of LON, tracing it from the extradural segment of C2 to its terminal branches in the skin. They highlighted LON's relationship with surrounding nerves and vascular structures, explaining its involvement in cervicogenic headaches.²⁴

In 1998, Becser et al²⁵ conducted an anatomic study of the occipital nerves to find suitable locations for nerve blocks. They found that the median distance from LON to the midline in the intermastoid line was 53 mm (range 32-90 mm). Also, Bahman Guyuron's study on 16 cadavers identified a block point for LON approximately 3 cm in diameter centered 6.5 cm from the midline and 5.3 cm below the line between the external auditory canals.²⁶

Compression or stretching along various LON trajectory areas can contribute to headache symptoms. Despite the anatomic variability observed, our study identifies M1 and M3 as reliable intervention points for LON, offering practical solutions for enhancing the precision and efficacy of nerve block procedures for

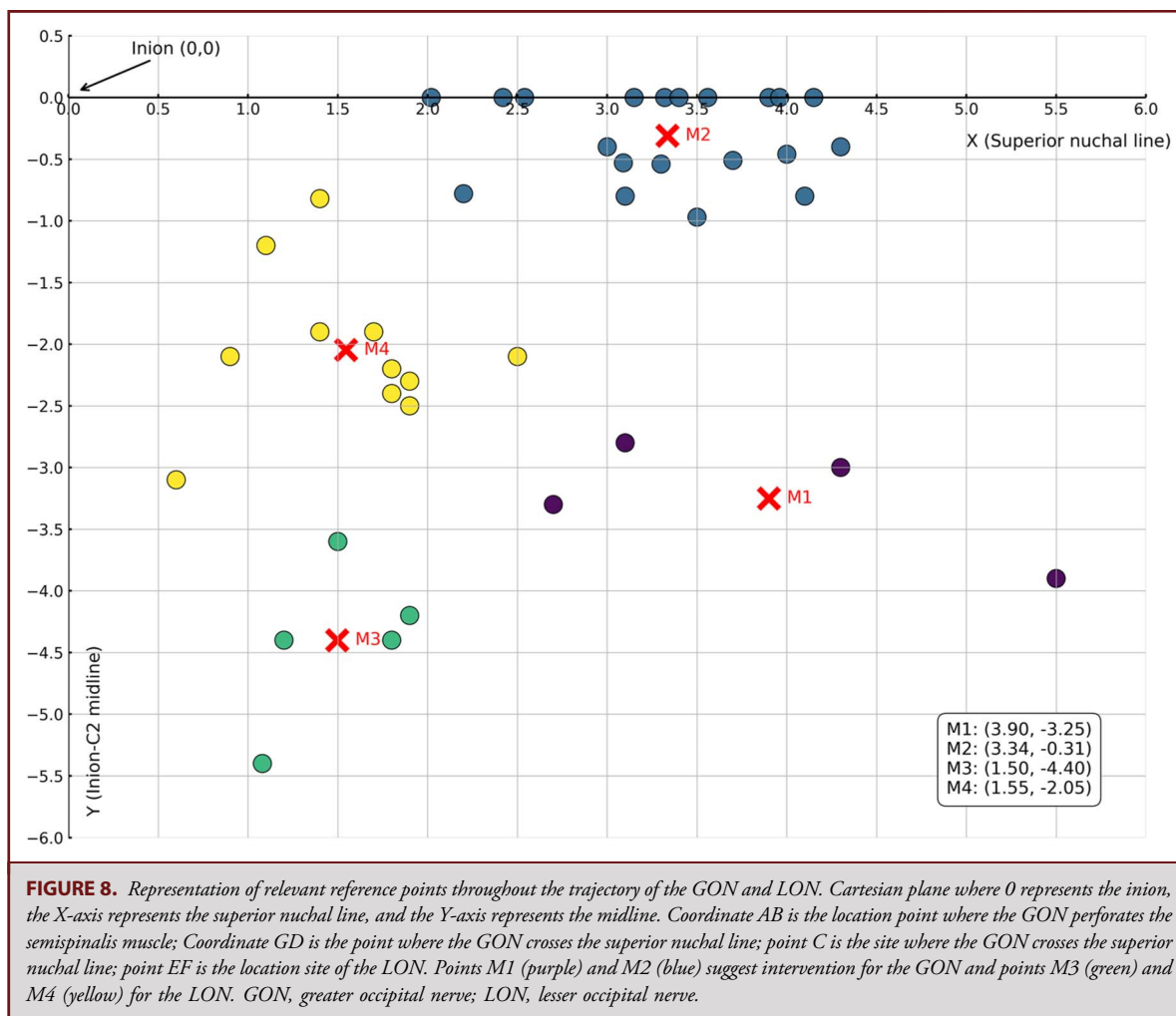
cervicogenic headaches. The K-means model clustered these points based on the spatial proximity of anatomic measurements rather than direct evidence of nerve compression.^{7,27} Although M1 and M3 do not exhibit overt compressive anatomy, they represent statistically common convergence zones for LON.

In clinical practice, percutaneous or open interventions (eg, nerve blocks, radiofrequency, or neuromodulation) often aim for predictable nerve locations rather than only the compression sites. This approach aligns with reports emphasizing that small, consistent anatomic targets can be more practical for pain procedures, especially when no clear compressive pathology is identified.^{15,28,29}

These insights into the anatomic locations of GON and LON and their respective block points underscore the importance of precise anatomic knowledge in planning effective treatments of occipital neuralgia and related headache disorders. Our findings align with previous studies but highlight challenges in determining precise intervention points because of significant anatomic variation observed in our sample. Unlike the relatively consistent measurements reported by Becser et al and Guyuron, our study suggests that LON pathway can vary considerably, complicating the identification of a consistent blocking point.^{25,26}

To address this, we propose 2 specific points for LON intervention: M1 and M3. M1 is strategically centered laterally to the C2-inion midline and below the superior nuchal line, offering a reliable reference point despite anatomic variations. On the other hand, M3, although presenting higher mean squared error rates compared with its GON counterparts, is within 2.5 cm from the observed site of LON. This proximity supports using M3 as a viable intervention point, consistent with the 3-cm radius proposed by Guyuron et al.²⁶

Furthermore, it is noteworthy that LON is less commonly implicated as a primary source of occipital neuralgia compared with GON, partly explaining the fewer identified points for LON



interventions. Still, these points (M1 and M3) remain clinically relevant for situations where LON is involved or where broader coverage of the occipital region is desired.^{19,30}

Finally, the imprecision of M1 and M3 from a purely surgical standpoint should not negate their potential utility for pain interventionists. Corticosteroid injections, diagnostic or therapeutic nerve blocks, and radiofrequency ablation rely on consistent surface landmarks and anatomic key points rather than surgically visualized compression sites.

These proposed points provide practical solutions for the anatomic variability encountered, potentially improving the accuracy and effectiveness of nerve block procedures for GON and LON.

LIMITATIONS AND FUTURE DIRECTIONS

The sample size, limited to 5 cadavers, restricts the extrapolation of these findings to broader populations. Although K-means clustering provided a framework for identifying anatomic coordinates of potential compression, morphological variability may affect the

reproducibility of these compression points in clinical practice. Finally, these findings stem from cadaveric dissections, which may not fully replicate physiological conditions in vivo. Future studies should include more specimens, integrate imaging techniques (MRI or ultrasound) in living subjects, and correlate anatomic and clinical data to refine therapeutic interventions.

CONCLUSION

This study provided a detailed description of the topological anatomy of the GON and LON and identified key areas and points along their trajectories. We propose, through an unsupervised AI model (K-means), 2 potential compression points for the GON: M2 (3.34 cm from the start of the superior nuchal line and 0.31 cm below it) and M4 (1.55 cm from the superior nuchal line and 2.05 cm below it). For the LON, the points are M1 (3.90 cm lateral to the C2-inion midline and 3.25 cm below the superior nuchal line) and M3 (1.50 cm from the superior nuchal line and 4.40 cm below it), which can improve the precision of corticosteroid injections and

nerve block procedures. These findings provide a valuable anatomic map for clinical practice, optimizing treatments of occipital neuralgia and associated headaches.

Funding

This study did not receive any funding or financial support.

Disclosures

The authors have no personal, financial, or institutional interest in any of the drugs, materials, or devices described in this article.

REFERENCES

- Natsis K, Baraliakos X, Appell HJ, Tsikaras P, Gigis I, Koebke J. The course of the greater occipital nerve in the suboccipital region: a proposal for setting landmarks for local anesthesia in patients with occipital neuralgia. *Clin Anat*. 2006;19(4):332-336.
- Gawel M, Rothbart P. Occipital nerve block in the management of headache and cervical pain. *Cephalalgia*. 1992;12(1):9-13.
- Brandt RB, Doesborg PGG, Meilof R, et al. Repeated greater occipital nerve injections with corticosteroids in medically intractable chronic cluster headache: a retrospective study. *Neurol Sci*. 2022;43(2):1267-1272.
- Vital JM, Grenier F, Dautheribes M, Baspeyre H, Lavignolle B, S n gas J. An anatomic and dynamic study of the greater occipital nerve (N. of Arnold). Applications to the treatment of Arnold's neuralgia. *Surg Radiol Anat*. 1989;11(3):205-210.
- Castillo-Rangel C, Gallardo-Garc a ES, Fadanelli-S nchez F, et al. Minimally invasive treatment of facet osteoarthritis pain in spine: a clinical approach evaluating cryotherapy. *World Neurosurg*. 2024;185:e741-e749.
- Castillo Rangel C, Marin G, Diaz Chiguer DL, et al. Radiofrequency cingulotomy as a treatment for incoercible pain: follow-up for 6 months. *Healthcare*. 2023;11(19):2607.
- Samsolsky Dekel BG, Sorella MC, Vasarri A, Melotti RM. The occipital nerves applied strain test to support occipital neuralgia diagnosis. *Pain Ther*. 2023;12(5):1135-1148.
- Platzgummer H, Moritz T, Gruber GM, et al. The lesser occipital nerve visualized by high-resolution sonography—normal and initial suspect findings. *Cephalalgia*. 2015;35(9):816-824.
- Guyuron B, Alessandri Bonetti M, Caretto AA. Comprehensive criteria for differential diagnosis and a surgical management algorithm for occipital neuralgia and migraine headaches. *JPRAS Open*. 2024;39:212-216.
- Ducic I, Moriarty M, Al-Attar A. Anatomical variations of the occipital nerves: implications for the treatment of chronic headaches. *Plast Reconstr Surg*. 2009;123(3):859-863.
- Saglam L, Coskun O, Gunver MG, Kale A, Gayretli O. An anatomical analysis of the occipital nerve complex: an essential tool for the application of occipital nerve blocks. *BMC Neurol*. 2024;24(1):308.
- Guo E, Gupta M, Sinha S, et al. neuroGPT-X: toward a clinic-ready large language model. *J Neurosurg*. 2024;140(4):1041-1053.
- Sammouda R, El-Zaart A. An optimized approach for prostate image segmentation using K-means clustering algorithm with elbow method. *Comput Intell Neurosci*. 2021;2021(1):4553832.
- Won HJ, Ji HJ, Song JK, Kim YD, Won HS. Topographical study of the trapezius muscle, greater occipital nerve, and occipital artery for facilitating blockade of the greater occipital nerve. *PLoS One*. 2018;13(8):e0202448.
- Saglam L, Coskun O, Gayretli O. Morphological and morphometric anatomy of the lesser occipital nerve and its possible clinical relevance. *Sci Rep*. 2024;14(1):5844.
- Janis JE, Hatef DA, Ducic I, et al. The anatomy of the greater occipital nerve: Part II. Compression point topography. *Plast Reconstr Surg*. 2010;126(5):1563-1572.
- Thomas DC, Chablani D, Parekh S, Pitchumani PK, Mallareddy SD, Mathai BC. Nerve and ganglion blocks in the management of headache disorders: a narrative review. *J Oral Maxillofac Anesth*. 2022;1:29.
- Blake P, Burstein R. Emerging evidence of occipital nerve compression in unremitting head and neck pain. *J Headache Pain*. 2019;20(1):76.
- Arata WH, Midha RK, Varrassi G, et al. Occipital nerve block for headaches: a narrative review. *J Oral Facial Pain Headache*. 2024;38(2):1-10.
- Busch V, Jakob W, Juergens T, Schulte-Mattler W, Kaube H, May A. Functional connectivity between trigeminal and occipital nerves revealed by occipital nerve blockade and nociceptive blink reflexes. *Cephalalgia*. 2006;26(1):50-55.

- Johansson A, Hao J, S j lund B. Local corticosteroid application blocks transmission in normal nociceptive C-fibres. *Acta Anaesthesiol Scand*. 1990;34(5):335-338.
- Bovim G, Bonamico L, Fredriksen TA, Lindboe CF, Stolt-Nielsen A, Sjaastad O. Topographic variations in the peripheral course of the greater occipital nerve. Autopsy study with clinical correlations. *Spine (Phila Pa 1976)*. 1991;16(4):475-478.
- Ashkenazi A, Levin M. Three common neuralgias. How to manage trigeminal, occipital, and postherpetic pain. *Postgrad Med*. 2004;116(3):16-48.
- De Ara ujo Lucas G, Laudanna A, Chopard RP, Raffaelli E. Anatomy of the lesser occipital nerve in relation to cervicogenic headache. *Clin Anat*. 1994;7(2):90-96.
- Becser N, Bovim G, Sjaastad O. Extracranial nerves in the posterior part of the head. Anatomical variations and their possible clinical significance. *Spine (Phila Pa 1976)*. 1998;23(13):1435-1441.
- Dash KS, Janis JE, Guyuron B. The lesser and third occipital nerves and migraine headaches. *Plast Reconstr Surg*. 2005;115(6):1752-1760.
- Ducic I, Felder JM, Khan N, Youn S. Greater occipital nerve excision for occipital neuralgia refractory to nerve decompression. *Ann Plast Surg*. 2014;72(2):184-187.
- Pillay P, Partab P, Lazarus L, Satyapal KS. The lesser occipital nerve in fetuses. *Int J Morphol*. 2012;30(1):140-144.
- Lee M, Brown M, Chepla K, et al. An anatomical study of the lesser occipital nerve and its potential compression points: implications for surgical treatment of migraine headaches. *Plast Reconstr Surg*. 2013;132(6):1551-1556.
- Cesmebasi A, Muhleman MA, Hulsberg P, et al. Occipital neuralgia: anatomic considerations. *Clin Anat*. 2015;28(1):101-108.

Acknowledgments

Author contributions: Conceptualization: GM, VF, JCPC, MB. Methodology: TOM, JSZC, DODR, VF, MB. Software: ATS. Validation: TOM, GM, CZC, VF, MB. Formal analysis: CZC, ATS. Investigation: TOM, JSZC, DODR. Data curation: CZC, TOM. Writing—original draft preparation: TOM, JSZC, CCR, CZC, PGLBB, ATS, DODR, VF. Writing—review and editing: GM, CCR, CZC, MB. Visualization: TOM, CZC, DODR. Supervision: GM, CCR, VF, MB.

Supplemental digital content is available for this article at operativeneurosurgery-online.com.

Supplemental Digital Content 1. Latex injection and instruments. This file details the protocol for latex injection, instruments used, and measurement landmarks (A–K).

Supplemental Digital Content 2. K-means methodology. This file explains the methodology for the K-means algorithm, clustering metrics, and elbow method.

COMMENTS

In this cadaveric study using 5 specimens, the authors dissected the greater and lesser occipital nerves and took various anatomic measurements. They used K-means clustering to identify optimal intervention points. Although the M1–4 points were consistent with previous studies, the authors noted that pinpointing precise intervention sites remains challenging, largely because of variability in the lesser occipital nerve. I concur with these limitations, as imaging—particularly ultrasound—could enhance the precision of treatments of both greater and lesser occipital nerve compression. This study may prove valuable for surgeons and pain specialists performing targeted nerve blocks or corticosteroid injections for greater occipital nerve compression.

Jason H. Huang

Temple, Texas, USA